Formation of hybrid parametric cavity polariton solitons

O. A. Egorov and F. Lederer

Institute of Condensed Matter Theory and Solid State Optics, Abbe Center of Photonics, Friedrich-Schiller-Universität Jena, Max-Wien-Platz 1, 07743 Jena, Germany

(Received 12 January 2013; revised manuscript received 12 March 2013; published 25 March 2013)

We study the nonlinear dynamics of exciton-polaritons in semiconductor microcavities operating in the strong-coupling regime and driven by a coherent optical pump above the exciton resonance. Provided that the exciton dispersion is accounted for, parametric mixing of polaritons from the upper and the lower polariton branches gives rise to modulational instability of the homogeneous solution. This instability leads to the formation of quasiperiodic patterns. Our analytical analysis shows that there are domains in parameter space where these patterns and stable homogeneous solution may exist simultaneously. This is the prerequisite for the existence of *cavity polariton solitons*—single-peak solutions on a homogeneous background. Because they originate from parametric mixing of polaritons from both branches of the dispersion relation we term them *hybrid parametric cavity solitons*. There are two kinds of these resting solitons—stationary and breathing ones. Both types require for stability that the cavity resonance be redshifted to the exciton resonance.

DOI: 10.1103/PhysRevB.87.115315 PACS number(s): 42.65.Pc, 71.36.+c, 42.65.Tg, 42.65.Sf

I. INTRODUCTION

The observation of strong coupling effects between excitons with a narrow linewidth and photons in planar high-quality semiconductor microcavities[1] opened a new era for investigations of nonlinear optical effects.[2,3] As a result of strong coupling new hybrid elementary coherent excitations, termed *exciton-polaritons*, may emerge. Their dispersion relation consists of an upper and lower branch, separated by the vacuum Rabi splitting. This is in strong contrast to semiconductor microcavities in the weak-coupling regime where intracavity photons interact incoherently and perturbatively with carriers and excitons.

The existence of exciton-polaritons results in extraordinary optical properties of these microcavities.[2,3] On the one hand Coulomb interactions among excitons evoke a strong and fast nonlinear response to an applied optical field. For instance, optical bistability was observed for an input power two orders of magnitudes less[4,5] than that required in the weak-coupling regime.[6] On the other hand the lower branch of the polariton dispersion relation, i.e., the dependence of the polariton frequency on the in-plane wave vector, has a peculiar nonparabolic shape with two inflection points where the effective polariton mass changes its sign. In particular, low-threshold parametric four-wave mixing can be achieved provided that the pump momentum exceeds a critical value and is incident at the "magic angle," i.e., at the inflection point.[7,8] Thanks to such properties, exciton-polariton based schemes are potential solutions to the most eminent problems that hinder the incorporation of nonlinear optics into real-world application, namely the weak and/or slow nonlinear response.

Very recent theoretical studies have shown that the interplay between polaritonic dispersion and strong excitonic nonlinearity allows also for the formation of a manifold of spatially localized, self-confined solutions, termed *cavity polariton solitons* (CPSs).[9–14] Because of the permanent energy exchange between the external pump and intrinsic losses they belong to the general class of dissipative solitons and are therefore strong attractors.[15] An intuitive physics behind the formation of some of these CPSs[9–11,14] goes back to the pioneering work on *cavity solitons* in the weak-coupling regime with parabolic dispersion.[6,16–19] Cavity solitons are either associated with locked switching fronts between two stable homogeneous solutions within their bistability domain[16] or appear near the region of modulation instability.[19]

However, the nonlinear dynamics of exciton-polaritons is involved. Frequently there are only minor analogies to conventional dissipative solitons. An example is the formation of two-dimensional moving CPSs near the inflection point of the dispersion relation. Apparently, parametric interaction between different spectral components of the CPS[12] can explain its stability and robust motion even for opposite signs of the polaritonic dispersion along two orthogonal directions. Recently these theoretical predictions[13] have been confirmed experimentally.[20]

In this paper we theoretically demonstrate the existence of two-dimensional cavity polariton solitons in semiconductor microcavities driven by an optical pump at a frequency fixed between the upper polariton branch and the excitonic resonance. This is in contrast to all other cavity polariton solitons which have been obtained in the direct vicinity of only one polariton branch (for a recent review see Ref. 14). We prove that the parametric interaction between polaritons on the upper and lower branch can give rise to the formation of stable hybrid localized solutions. In Sec. II we put forward the mathematical model and discuss both the polaritonic dispersion and the properties of homogeneous nonlinear solutions. Then, in Sec. III, we perform an analytical analysis of this parametric interaction. In particular, the conditions for the coexistence of a stable homogeneous solution and a periodic pattern will be discussed. In Sec. IV we derive the existence domain of hybrid parametric cavity polariton solitons and study their stability. It will turn out that there are stable stationary solitons; however, usually they undergo a Hopf instability and develop into stable oscillating solutions, referred to as *breathing solitons* or *polariton breathers*. Furthermore, it appears that nonzero excitonic dispersion is required for the existence of both stationary and breathing hybrid parametric solitons.

II. MATHEMATICAL MODEL

We start by introducing the widely accepted dimensionless model for excitons strongly coupled to cavity photons:[2,3,10,11,14]

$$\begin{aligned} \partial_t E - i\nabla_\perp^2 E + [\gamma - i(\Omega_P + \delta)]E &= i\Psi + E_p, \\ \partial_t \Psi - i d\nabla_\perp^2 \Psi + (\gamma - i\Omega_P)\Psi + i|\Psi|^2\Psi &= iE. \end{aligned} \tag{1}$$

Here, E and Ψ are the averages of the photon and exciton creation or annihilation operators and polarization effects are disregarded. The normalization is such that $(\Omega_R/g)|E|^2$ and $(\Omega_R/g)|\Psi|^2$ are the photon and exciton numbers per unit area, Ω_R is the Rabi frequency directly related to the atom-field coupling strength, and g is the exciton-exciton interaction constant. The quantity $\Omega_P = (\omega_P - \omega_0)/\Omega_R$ describes the detuning of the pump frequency (ω_p) from the excitonic resonance (ω_0) at $k = 0$. We also permit a frequency mismatch between the excitonic and the cavity (ω_c) resonance at $k = 0$: $\delta = (\omega_0 - \omega_c)/\Omega_R$. The time t is measured in units of $1/\Omega_R$. The cavity and the exciton damping constants are assumed to be equal (γ) and normalized to Ω_R. The transverse coordinates x, y are normalized to the value $x_0 = \sqrt{c/2k_0 n\Omega_R}$ where c is the vacuum light velocity, n is the effective refractive index of the cavity, and $k_0 = n\omega_p/c$ is the length of the wave vector. The normalized amplitude of the external pump E_p is related to the incident intensity $I_{\rm inc}$ as $|E_p|^2 = g\gamma I_{\rm inc}/\hbar\omega_p\Omega_R{}^2$.[8]

Here we are taking into account the parabolic dispersion (effective mass approach) of the excitons where the exciton dispersion coefficient is normalized to the photon diffraction coefficient as $d = \hbar\omega_c n^2/m_{\rm exc}c^2$, where $m_{\rm exc}$ is the effective exciton mass. Realistically it holds $d \sim 10^{-4}$ to 10^{-5}.

As a guideline for realistic estimates one can use parameters of a microcavity with a single InGaAs/GaAs quantum well: $\hbar\Omega_R \simeq 2.5$ meV, $\hbar g \simeq 10^{-4}$ eV μm^2; see Refs. 4 and 21. Therefore, a unit of t corresponds to 0.25 ps and a unit of x to $x_0 \sim 1$ μm. Assuming the relaxation times of excitons and the cavity lifetime to be 2.5 ps gives $\gamma \simeq 0.1$. In accordance with this set of parameters the normalized driving amplitude $|E_p|^2 = 1$ corresponds to an external pump intensity of about 6 kW/cm^2.

First, we briefly discuss the linear polariton dispersion, which is defined as the dependence of the frequency $\Omega(k) = [\omega(k) - \omega_0]/\Omega_R$ on the in-plane momentum $k^2 = k_x^2 + k_y^2$. Looking for a solution as

$$\{E(t,x,y), \Psi(t,x,y)\} = \vec{p}_k e^{-\gamma t + i[(k_x x + k_y y) - \Omega(k)t]}$$

and dropping both the pump and the nonlinear term, one finds the eigenvalue problem for the basis vector $\vec{p}_k = \{e_k, \psi_k\}$ and the eigenfrequency $\Omega(k)$ (for details see Ref. 12). Here, e_k and ψ_k are the amplitudes of the photonic and excitonic components (also known as the Hopfield coefficients[22]), respectively. A solution of the eigenvalue problem yields the two branches of the linear polariton dispersion relation

$$\Omega_\pm(k) = \frac{(1+d)k^2 - \delta}{2} \pm \sqrt{1 + \frac{[(1-d)k^2 - \delta]^2}{4}}, \tag{2}$$

where the $+$ and $-$ signs refer to the upper and lower branches, respectively. For $\delta, k = 0$ we get $\Delta\Omega = \Omega_+(0) - \Omega_-(0) = 2$ (or $\Delta\omega = 2\Omega_R$), representing the Rabi splitting, i.e., the separation of the two branches of the dispersion curve in the center ($k = 0$) and for identical excitonic and photonic resonances ($\omega_0 = \omega_c$). The ratio of photonic and excitonic component of the polariton can be found from the eigenvector $\vec{p}_k$ as

$$e_k/\psi_k = \Omega_\pm(k) - dk^2. \tag{3}$$

In the case considered in this paper, the separation of both branches and the location of their centers depend additionally on the mismatch δ [see Eq. (2) and Fig. 1(a)]. This will be essential for the effects dealt with below. The lower polariton branch converges to the pure excitonic one with parabolic dispersion for very large momenta [see right part in Fig. 1(a) for $k > 10$].

Moving or resting cavity polariton solitons may exist very close to either the lower[9,10,13] or upper[11] polariton branches. These CPSs are localized objects on a finite-amplitude background which is a steady-state *homogeneous solution* (HS) of the governing equations. It turned out that the bistable behavior of the HS with respect to the pump amplitude is a prerequisite for the existence of these CPSs (see Refs. 9–11, and 13 or for a recent review Ref. 14). To find the amplitude (E) of the HS we are looking for a spatially uniform solution of the stationary version of Eq. (1) with vanishing spatial derivatives ($\partial_t = 0$ and $\nabla_\perp^2 = 0$). It can be proven[9,14] that the HS $E(E_p)$ is bistable provided that $f(\Omega_p) > 0$, where

$$f(\Omega_p) \equiv (\Omega_p - \sqrt{3}\gamma)[\gamma^2 + (\Omega_p + \delta)^2] - (\Omega_P + \delta + \sqrt{3}\gamma).$$

In contrast to the previous cases, we choose the operating frequency within the gap between the excitonic resonance and the upper polariton branch. This choice of parameters results in a monostable response of the HS because of $f(\Omega_P) < 0$. Figures 1(b) and 1(c) show both the photonic and the excitonic component of the monostable HS. By virtue of linear stability analysis we found that the HS becomes *modulationally*

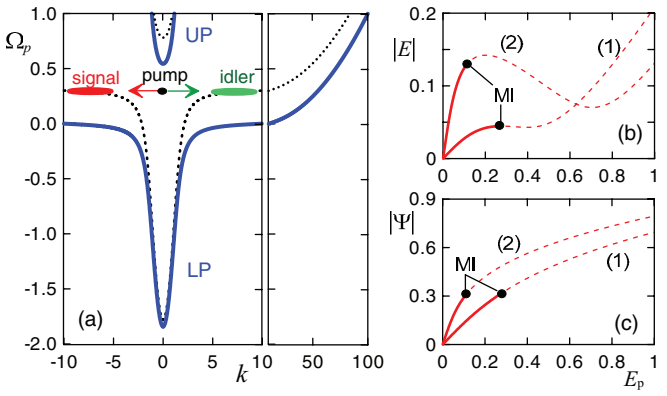

FIG. 1. (Color online) (a) The frequency of exciton-polaritons vs their in-plane momentum k (dispersion curves). The momentum k is expressed in units of x_0^{-1}. "LP" and "UP" designate the lower and upper polariton branches, respectively. The nonlinear dispersion relation is also shown (dashed lines). The right part shows the excitonic dispersion for large k. (b) Photonic and (c) excitonic components of the nonlinear homogeneous solution (HS) vs the optical pump amplitude for different operating frequencies: (1) for $\Omega_P = 0.2$, (2) for $\Omega_P = 0.5$. MI: Bifurcation point of modulational instability. Parameters: $\delta = 1.3$, $\gamma = 0.1$, $d = 10^{-4}$.

unstable if the pump amplitude exceeds a critical value [see MI in Figs. 1(b) and 1(c)]. As usual, modulational instability (MI) is understood as the growth of linear modulated perturbations in the form $\sim\exp\left(ik_x x + ik_y y + \lambda t\right)$ where Reλ is the growth rate. The HS is modulationally unstable for Re$\lambda > 0$. As we show below the parametric mixing of polaritons from the upper and lower branch evokes this instability.

III. PARAMETRIC MIXING OF POLARITONS FROM THE UPPER AND LOWER BRANCH

Provided that the operating frequency exceeds the exitonic resonance ($\Omega_P > 0$) and the photonic resonance is redshifted to the excitonic one ($\delta > 0$), the optical pump is closer to the upper polariton branch. Thus the upper branch polaritons contribute mostly to the homogeneous solutionat $k = 0$ and the pump frequency $\Omega(0) = \Omega_P$, indicated as "pump" in Fig. 1(a). This homogeneous solution interacts parametrically with polaritons at the blueshifted lower polariton branch [indicated as "signal" and "idler" in Fig. 1(a)], provided that the pump amplitude exceeds some critical value. Indeed, the resonant scattering of two upper branch polaritons (excited by the frequency detuned pump at $k_p = 0$) into the signal (k_s) and idler ($k_i = -k_s$) polariton of the lower polariton branch evokes the modulational instability of the HS [see Fig. 1(a)]. To understand the dynamics of the signal and idler waves near the parametric threshold we express E and Ψ in Eq. (1) as

$$E(x,y,t) = E_0 + A(t)(e_s/\psi_s)(e^{i(k_{sx}x+k_{sy}y)} + e^{-i(k_{sx}x+k_{sy}y)}),$$
$$\Psi(x,y,t) = \Psi_0 + A(t)(e^{i(k_{sx}x+k_{sy}y)} + e^{-i(k_{sx}x+k_{sy}y)}), \quad (4)$$

where $k_s = \sqrt{k_{sx}^2 + k_{sy}^2}$. Here $A(t)$ is the identical slowly varying complex amplitude of both the signal and idler wave. e_s and ψ_s are the components of $\vec{p}_k$ for $k = k_s$. Inserting the ansatz (4) into Eq. (1) one obtains the amplitude equation (for details, see Ref. 12):

$$i\frac{\partial A}{\partial t} + [i\gamma + \Delta_s(k_s)]A - \xi(2|\Psi_0|^2 + 3|A|^2)A - \xi\Psi_0^2 A^* = 0, \quad (5)$$

where $\Delta_s(k_s) = \Omega_p - \Omega_-(k_s)$ is the effective frequency detuning of the signal/idler polariton from the LP branch and $\xi = |\psi_s|^2/(|e_s|^2 + |\psi_s|^2)$ is the nonlinear interaction coefficient.

First, we discuss briefly the parametric threshold for the generation of small signal and idler polaritons in the undepleted pump approximation ($|\Psi_0| \gg |A|$). Looking for the solution of Eq. (5) in the form $A(t) = ae^{\lambda t}$ and $A^*(t) = be^{\lambda t}$ for the constant HS amplitude Ψ_0 and keeping only linear terms in the fluctuations a and b, one gets the solution of the eigenvalue problem for λ:

$$\text{Re}\lambda(k_s) = -\gamma \pm \sqrt{\xi^2|\Psi_0|^4 - [\Delta_s(k_s) - 2\xi|\Psi_0|^2]^2}. \quad (6)$$

The HS becomes modulationally unstable provided that the real part of the eigenvalue is positive (Re$\lambda > 0$). The growth rate (Reλ) of the unstable modulated perturbation is plotted as a function of the momentum k_s and the modulus of the HS $|\Psi_0|$ in Fig. 2(a). Identical result have been obtained by a direct linear stability analysis of the HS in the original model [Eq. (1)].

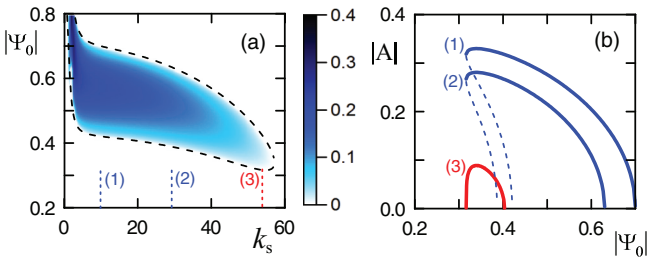

FIG. 2. (Color online) (a) Growth rate of the perturbation [real part of λ in Eq. (6)] as a function of the modulus of the homogeneous excitonic component $|\Psi_0|$ and the momentum k_s. The dashed line depicts the analytical results Eq. (7) for the parametric threshold. (b) Signal amplitude $A(k_s)$ [see Eq. (8)] vs the modulus of the homogeneous excitonic component $|\Psi_0|$ calculated for different momenta: (1) $k_s = 10 \rightarrow \Delta_s = 0.5$; (2) $k_s = 30 \rightarrow \Delta_s = 0.41$; (3) $k_s = 55 \rightarrow \Delta_s = 0.198$. Solid (dashed) lines: Stable (unstable) solutions. Other parameters: $\Omega_P = 0.5$, $\delta = 1.3, \gamma = 0.1, d = 10^{-4}$.

The parametric threshold can be defined as Re$\lambda(|\Psi_0|) = 0$ where modulational instability of the trivial signal and idler states just sets in. This threshold is then given by

$$|\Psi_{\text{MI}}(k_s)|^2 = \frac{2\Delta_s(k_s) \pm \sqrt{\Delta_s{}^2(k_s) - 3\gamma^2}}{3\xi}. \quad (7)$$

Parametric gain exists in a very wide k_s interval which can exceed the maximal value of the pure photonic dispersion relation [see Fig. 1(a) for $k > 10$]. Thus, for very large momenta the dispersion of the lower polariton branch coincides essentially with that of excitons $\Omega_-(k_s) \approx dk_s^2$. In this case the maximal momentum for parametric gain can be simply derived from the Eq. (7) as $k_{s\,\max}^2 \sim (\Omega_p - \sqrt{3}\gamma)d^{-1}$. It is evident that the maximal momentum $k_{s\,\max}$ becomes infinite in the limit of vanishing excitonic dispersion.

The steady-state solution of Eq. (5) provides nontrivial solutions for the amplitude of the signal/idler wave in the undepleted pump approximation:

$$|A_\pm(k_s)|^2 = \frac{-2\xi|\Psi_0|^2 + \Delta_s(k_s) \pm \sqrt{\xi^2|\Psi_0|^4 - \gamma^2}}{3\xi}. \quad (8)$$

These nontrivial solutions emanate from bifurcation points [see Eq. (7)], as shown in Fig. 2(b). The bifurcation is subcritical provided that the frequency detuning exceeds the critical value $\Delta_s(k_s) = \Omega_P - \Omega_-(k_s) > 2\gamma$. In this case for identical $|\Psi_0|$ simultaneously stable trivial and nontrivial solutions exist which is a first indication for the potential existence of stable patterns and bright solitons. This condition for subcritical bifurcation is satisfied in a wide momentum range k_s except a tiny region near $k_{s\,\max}$ [see Fig. 2(b)].

Summarizing these analytical results one expects that stable periodical patterns can coexist with a homogeneous steady-state solution, at least in the undepleted pump approximation, provided that the operating frequency is above the excitonic resonance and satisfies $\Omega_p > 2\gamma$.

To numerically prove this we used a HS with some noise added as the initial condition and calculated the field evolution in the original model (1) for a pump amplitude slightly above the parametric threshold ($E_{\text{th}} \approx 0.29$). In accordance with Eq. (6), perturbations with a wide range of respective momenta

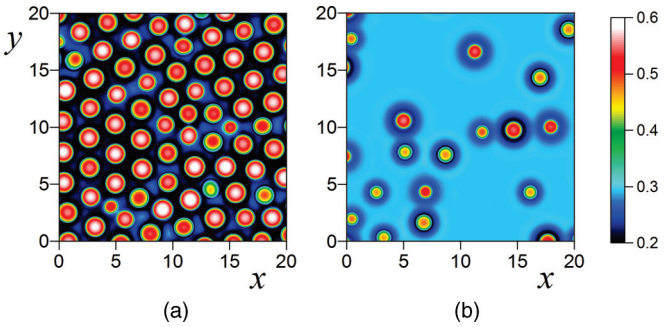

FIG. 3. (Color online) The excitonic component of the polariton for different pump powers. (a) Snapshot of a "breathing" pattern slightly above the parametric threshold ($E_p = 0.3$). (b) Snapshot of "breathing" localized solutions below the parametric threshold ($E_p = 0.25$). The pattern (a) has been used as an initial condition. Other parameters: $\Omega_P = 0.2$, $\gamma = 0.1$, $\delta = 1.3$, $d = 10^{-4}$.

k_s experience the parametric amplification. This results in the formation of quasiperiodic patterns with oscillating peaks [Fig. 3(a)]. Then we performed calculations for the pump amplitude below the parametric threshold with the previous pattern as the initial condition. It turned out that some of the peaks survive on a stable homogeneous background forming oscillating localized solutions [Fig. 3(b)]. The existence conditions and stability properties of these localized solutions will be discussed in the succeeding section.

IV. EXISTENCE AND STABILITY OF POLARITON SOLITONS

Direct numerical simulations in the original model (1) showed that stable bright self-localized polariton states, i.e., cavity polariton solitons (CPS), may exist just below the boundary of the modulational instability (MI) domain associated with parametric mixing between polaritons of the upper and lower branches. The profile of the photonic and excitonic components of these CPSs are shown in Figs. 4(a) and 4(d), respectively. The CPS branch bifurcates subcritically from the boundary of the MI domain [see CPS branches in Figs. 4(c) and 4(d)]. It is known from a previous study[11] that nonlinear coupling to almost free excitons with large momenta can destabilize the CPSs existing within the polaritonic gap. To probe the stability of the CPSs profile $(E_{st}(x,y),\Psi_{st}(x,y))$ against weak perturbations we performed a standard linear stability analysis of the model (1). Looking for the solution close to the stationary one in the form $E(x,y,t) = E_{st}(x,y) + \partial e(x,y)e^{\lambda t}$ and $\Psi(x,y,t) = \Psi_{st}(x,y) + \partial\psi(x,y)e^{\lambda t}$ we calculated the growth rates of the small perturbations $\partial e(x,y)$, $\partial\psi(x,y)$. We found that being stable for smaller values of the pump amplitudes close to the turning point the major part of the entire soliton branch is unstable against a Hopf instability which implies a complex value of the growth rate $\mathrm{Im}\lambda \neq 0$ [see Figs. 4(c) and 4(d)]. For a nonzero realistic excitonic dispersion ($d \approx 10^{-4}$) the Hopf instability develops into periodic oscillations between the maximal and minimal values [solid lines in Figs. 4(c) and 4(d)]. The branch of dynamically stable oscillating CPSs or *polariton breathers* bifurcates from the branch of stable CPSs.

Evidence of parametric mixing between polaritons with different momenta (pump, signal, and idler) can be traced in the spectrum of stable CPSs [Fig. 5(a)]. Indeed, the spectrum of the excitonic component contains two maxima at nonzero momenta which can be regarded as the signal ($k \approx k_s$) and the idler ($k \approx -k_s$) polaritons. The signal momentum roughly

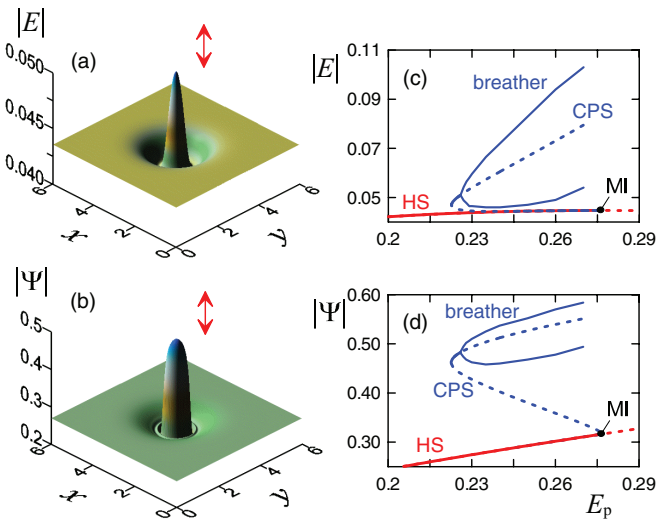

FIG. 4. (Color online) Photonic (a) and excitonic (b) components of the two-dimensional CPS profile for $E_p = 0.225$. The photonic (c) and excitonic (d) components of the CPS branches vs the optical pump amplitude. The dashed lines correspond to unstable CPSs. The breathing CPS profile oscillates between the maximal and minimal values shown in the figure. Other parameters: $\Omega_P = 0.2$, $\gamma = 0.1$, $\delta = 1.3$, $d = 10^{-4}$.

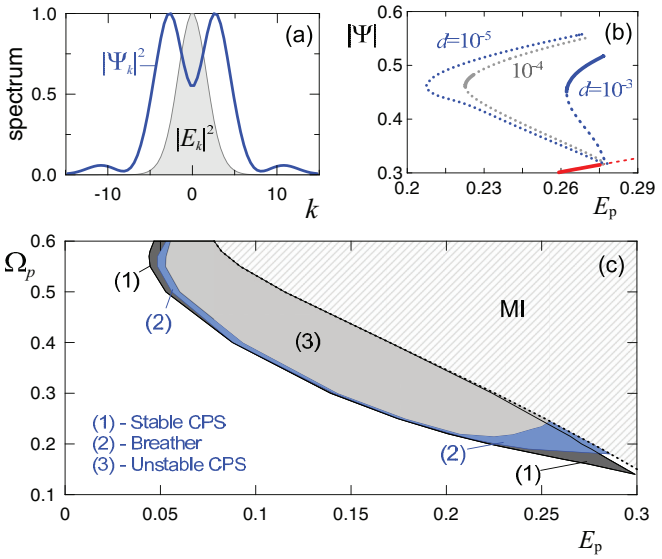

FIG. 5. (Color online) (a) Photonic and excitonic components in momentum space for the CPS displayed in Fig. 4. (b) Modulus of the maximum of the excitonic component of the CPSs branch ($\Omega_P = 0.2$) for different values of the excitonic dispersion: $d = 10^{-5}$, $d = 10^{-4}$, and $d = 10^{-3}$. (c) Existence domain of stable CPSs and polariton breathers as function of the pump amplitude E_p and the pump frequency Ω_p. The value $d = 10^{-4}$ was used for these calculations. "MI" marks the modulationally unstable domain of the HS. Other parameters: $\gamma = 0.1$, $\delta = 1.3$.

corresponds to the momentum of maximal parametric gain of a HS given by Eq. (6) and shown in Fig. 2(a). In accordance with Eq. (3) the photonic contribution to the hybrid polaritons decreases monotonically with k. Thus the photonic component of the CPS spectrum drops faster than the excitonic one for increasing k [Fig. 5(a)]. We note that the overwhelming part of the soliton spectrum is bounded within the domain of the polariton dispersion relation where the photonic component does not vanish [i.e., $k \lesssim 10$ in Fig. 1(a)]. Under these circumstances the additional relaxation mechanism associated with the scattering of polaritons at acoustic phonons can be neglected.[23]

It turns out that the excitonic dispersion plays the primary role as far as the existence domain and the stability of these hybrid CPSs are concerned. Indeed, their existence interval regarding the pump amplitude is maximal for the nondispersive case ($d < 10^{-5}$) and decreases gradually with increasing d [Fig. 5(b)]. This result is also in qualitative agreement with the analytical analysis of the nontrivial parametric solution given by Eq. (8). The signal bifurcates supercritically provided that the excitonic dispersion becomes unrealistically large $d > 0.01$. On the contrary a nonzero excitonic dispersion can stabilize the CPSs which are usually unstable and undergo strong oscillations for vanishing excitonic dispersion [compare the cases $d = 10^{-5}$ and 10^{-3} in Fig. 5(b)]. For our choice of the cavity-exciton mismatch ($\delta = 1.3$), a realistic excitonic dispersion ($d = 10^{-4}$) corresponds to the intermediate case where the oscillatory instability of the CPS is sufficiently weak. Thus the formation of both periodically oscillating and stationary CPSs becomes feasible. Note that the CPSs can be further stabilized by an increased redshift of the cavity resonance with respect to the excitonic one (increasing δ).

Intensive numerical simulations based on the original model (1) showed that hybrid CPSs exist for pump frequencies situated in a region between the upper polariton branch and a minimal value of $\Omega_p \approx 1.5\gamma$, as shown in Fig. 5(c). Tuning the operating frequency off the excitonic resonance reduces substantially the pump amplitude required for soliton formation. Moreover, disregarding the oscillatory instability (which can be lifted by other parameters), the existence interval of hybrid parametric CPSs can be as large as half of the pump amplitude itself [Fig. 5(c)]. It reaches a minimal value for the operating frequency crossing the upper polariton branch ($\Omega_p \approx 0.57$). In this case the optical pump excites resonantly the upper polariton branch which interacts with polaritons of the lower branch. Here parametric mixing gives rise to a hybrid CPS with an unusual non-bell-shape [Figs. 6(a) and 6(b)]. The spot size of the excitonic component is at least four times smaller than the photonic one and is about 2 μm. Hence, because the (nonlinear) excitonic component plays the major role with regard to interactions between CPSs the minimal distance between solitons can be quite small. This could be attractive for future implementation of this type of CPS in compact devices.[6]

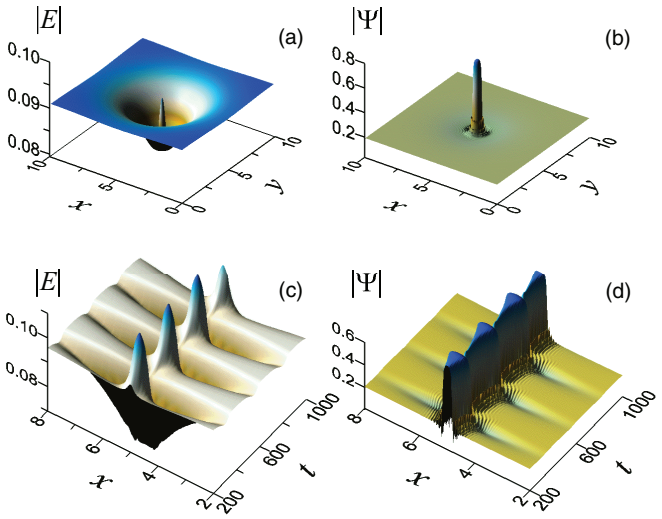

FIG. 6. (Color online) Moduli of the photonic (a) and excitonic (b) components of the two-dimensional stable CPS profile for $E_p = 0.055$. Evolution of the photonic (c) and excitonic (d) components of the breathing CPS for $E_p = 0.06$. Other parameters: $\Omega_p = 0.5$, $d = 10^{-4}$, $\gamma = 0.1$, $\delta = 1.3$.

Figures 6(c) and 6(d) show an example of strongly oscillating hybrid CPSs slightly above the Hopf instability threshold. Depending on the detuning Ω_P, the oscillation period varies between twenty and fifty polariton lifetimes, which correspond to about 50–125 picoseconds. The oscillations may lead to the disintegration of the breathing CPS provided that the pump amplitude is substantially larger than the instability threshold.

V. CONCLUSION

We have provided a detailed analytical and numerical analysis of cavity polariton solitons which are forming due to parametric mixing of polaritons of the upper and lower branch in a planar semiconductor microresonator operating in the strong-coupling regime. These hybrid solitons exist provided that the frequency of the optical pump is situated between the excitonic resonance and the upper polariton branch. Both a redshift of the cavity resonance with regard to the exciton resonance and a nonzero excitonic dispersion are required for the stable formation of both resting stationary and breathing cavity polariton solitons. Surprisingly these hybrid parametric CPSs require even less pump power than CPSs previously obtained excited close to exclusively one of the polariton branches.[9–14]

[1] C. Weisbuch, M. Nishioka, A. Ishikawa, and Y. Arakawa, Phys. Rev. Lett. **69**, 3314 (1992).

[2] B. Deveaud, *Physics of Semiconductor Microcavities* (Wiley-VCH, Weinheim, 2007).

[3] A. Kavokin, J. Baumberg, G. Malpuech, and F. Laussy, *Microcavities* (Oxford University Press, New York, 2007).

[4] A. Baas, J. P. Karr, H. Eleuch, and E. Giacobino, Phys. Rev. A **69**, 023809 (2004).

[5]D. Bajoni, E. Semenova, A. Lemaitre, S. Bouchoule, E. Wertz, P. Senellart, S. Barbay, R. Kuszelewicz, and J. Bloch, Phys. Rev. Lett. **101**, 266402 (2008).
[6]T. Ackemann, W. J. Firth, and G. L. Oppo, Adv. At. Mol. Opt. Phys. **57**, 323 (2009).
[7]D. M. Whittaker, Phys. Rev. B **71**, 115301 (2005).
[8]M. Wouters and I. Carusotto, Phys. Rev. B **75**, 075332 (2007).
[9]A. V. Yulin, O. A. Egorov, F. Lederer, and D. V. Skryabin, Phys. Rev. A **78**, 061801(R) (2008).
[10]O. A. Egorov, D. V. Skryabin, A. V. Yulin, and F. Lederer, Phys. Rev. Lett. **102**, 153904 (2009).
[11]O. A. Egorov, D. V. Skryabin, and F. Lederer, Phys. Rev. B **82**, 165326 (2010).
[12]O. A. Egorov, D. V. Skryabin, and F. Lederer, Phys. Rev. B **84**, 165305 (2011).
[13]O. A. Egorov, A. V. Gorbach, F. Lederer, and D. V. Skryabin, Phys. Rev. Lett. **105**, 073903 (2010).
[14]O. A. Egorov, D. V. Skryabin, and F. Lederer, Springer Ser. Opt. Sci. **170**, 171 (2012).
[15]N. Akhmediev and A. Ankiewicz, *Dissipative Solitons* (Springer, Berlin, 2005).
[16]N. Rosanov, *Spatial Hysteresis and Optical Patterns* (Springer, Berlin, 2002).
[17]D. Michaelis, U. Peschel, and F. Lederer, Phys. Rev. A **56**, R3366 (1997).
[18]M. Brambilla, L. A. Lugiato, F. Prati, L. Spinelli, and W. J. Firth, Phys. Rev. Lett. **79**, 2042 (1997).
[19]U. Peschel, D. Michaelis, and C. O. Weiss, IEEE J. Quantum Electron. **39**, 51 (2003).
[20]M. Sich, D. Krizhanovskii, M. S. Skolnick, A. V. Gorbach, R. Hartley, D. Skryabin, E. Cerda-Mendez, K. Biermann, R. Hey, and P. Santos, Nat. Photonics **6**, 50 (2012).
[21]I. Carusotto and C. Ciuti, Phys. Rev. Lett. **93**, 166401 (2004).
[22]J. J. Hopfield, Phys. Rev. **112**, 1555 (1958).
[23]F. Tassone, C. Piermarocchi, V. Savona, A. Quattropani, and P. Schwendimann, Phys. Rev. B **56**, 7554 (1997).